186

A Distributed Temperature Sensor Based on Liquid-Core Optical Fibers

ARTHUR H. HARTOG

Abstract—**The principles of operation, the design, and performance of a fiber-optic temperature-distribution sensor are discussed. The sensor uses optical time-domain reflectometry (OTDR) to detect temperature-induced changes of backscatter power at many separate locations in the fiber. In liquid-core fibers, a sensitivity of 2.3×10^{-2} dB/°C (0.54 percent $°C^{-1}$) was observed. A measurement accuracy of 1°C with a spatial resoltuion of 1 m is attainable over a fiber length of 100 m.**

I. Introduction

OPTICAL-FIBER SENSORS [1], [2] are the subject of considerable interest and devices have been proposed for the measurement of a large number of physical parameters including temperature [3]-[5], acoustic, electric and magnetic fields, pressure, strain rotation, and displacement. They have been reviewed extensively in [1] and [2]. Optical-fiber sensors are of advantage for remote measurements in environments which are hazardous or which suffer from severe electromagnetic interference or where space and weight are restricted. Sensors consisting entirely of optical fibers can be considerably more rugged than bulk transducers and although the sensitivity of glasses to external influences is usually lower than that of suitable crystals, this may often be compensated by the longer path lengths available in fibers.

Optical-fiber sensors presented to date modify either the intensity, the phase, the state-of-polarization, or the time-of-flight of the light traveling in the fiber [1], [2]. Elaborate techniques have been employed, especially in the case of the gyroscope [1], to reduce the transducer's sensitivity to factors other than that to be measured. In most cases, the measured value refers either to a specific location in space or to some form of average of the sensed quantity over the entire length of fiber sensor [3], [4]. It is then not possible to gain information about the spatial distribution of the measured value without resorting to multiple sensors.

In the present paper, a new class of fiber-optic sensors is proposed which are able to monitor the physical quantity of interest at many points along the fiber simultaneously. The sensors are based on optical time-domain reflectometry (OTDR) in specially designed fibers. OTDR is a well-known [6], [7] technique for observing length-dependent changes in fiber parameters [8]-[12]. In order to use this technique in a fiber sensor, the fiber must be designed in such a way that

Manuscript received April 12, 1983. This work was financially supported by the UK Science and Engineering Research Council.

The author is with the Department of Electronics, The University, Southampton, Hampshire, S09 5NH, England.

0733-8724/83/0900-0498$01.00

its backscatter signature is sensitive to the external physical parameter to be monitored.

The proposed technique may be seen as an extension of polarization OTDR [13], [14] where changes in the state of polarization (which is affected by external factors) along a single-mode fiber are sensed using OTDR. In the present sensors, changes in scattering loss, numerical aperture (NA), or total attenuation may be used to provide the required sensitivity.

The sensors may be classed with other intensity-modulating transducers but they use timing information to multiplex the values sensed at many separate locations onto the one fiber.

In this paper, these ideas are applied to the development of a temperature-distribution sensor using liquid-core fibers which are known to exhibit a large sensitivity of Rayleigh scattering loss and NA to temperature changes.

II. Theory of Operation

A. Review of OTDR

The basic arrangement of OTDR [6], [7] is shown in Fig. 1. A laser is used to launch short optical pulses into the fiber via a directional coupler. As the pulse travels along the fiber, it is attenuated via several mechanisms, one of which is Rayleigh scattering. Some of the light thus scattered is guided by the fiber back to the launching end where it is detected by the receiver. The resulting waveform takes the shape of a decaying pulse since the forward-traveling pulse and that portion of the light which is scattered backwards are both attenuated by propagation along the fiber.

The scattered power $p(t)$ returning to the launching end after time t is given by

$$p(t) = P_0 \, W \eta(z) \exp - \int_0^t \alpha(z) \, v_g \, dt \qquad (1)$$

where P_0 is the power launched into the fiber, W the pulsewidth, v_g the group velocity, $\alpha(z)$ the local attenuation coefficient, and $\eta(z)$ the backscatter factor, i.e., the ratio of the backscatter power to the probe pulse energy. Distance z from the launching end is related to elapsed time t via $z = v_g t/2$. In the case of a multimode step-index fiber η may be expressed as [15]

$$\eta = \frac{1}{2} \alpha_s v_g S = \frac{1}{2} \alpha_s v_g \frac{3}{8} \frac{n_1^2 - n_2^2}{n_1^2} \qquad (2)$$

where α_s is the Rayleigh scattering loss coefficient and S is the capture fraction, i.e., the proportion of the scattered light which is recaptured by the waveguide. In step-index multimode fibers, S is determined purely by the core, and cladding refractive indexes (n_1 and n_2, respectively).

In a fiber which is uniform along its length, the backscatter signal takes the form of a decaying exponential (see (1)), the rate of decay being determined by the attenuation of the fiber. In practice, backscatter waveforms are found to depart from the expected behavior owing to longitudinal variations in fiber parameters [8]-[12], [16]. Fig. 2 shows an example of a nonexponential backscatter waveform; in this case, the increase

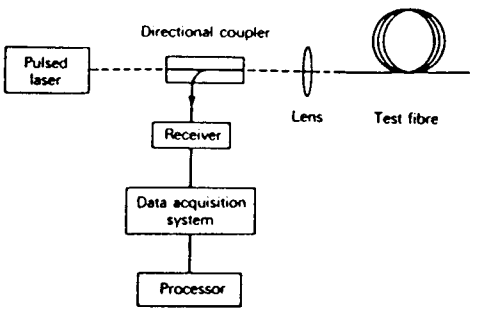

Fig. 1. Functional diagram of an optical time-domain reflectometer.

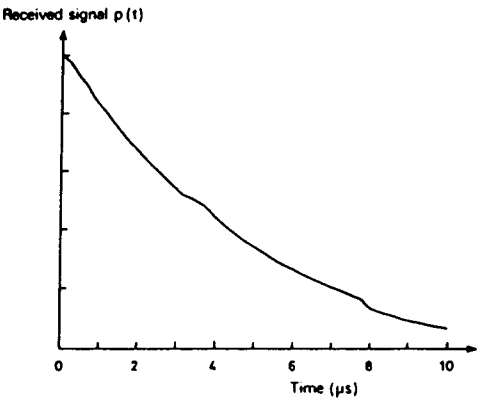

Fig. 2. Backscatter waveform obtained on a multimode fiber having a nonuniform diameter.

in signal in the central section of the fiber is caused by a 12-percent reduction in fiber diameter. Fiber-diameter variations are the most common cause for the features of backscatter signatures in multimode fibers since they strongly alter the modal power distribution [9], [16]. In addition, according to (1) and (2), a longitudinal change of the Rayleigh scatter coefficient or of the NA will have a direct influence on the backscatter level, and the rate-of-decay is affected by variations in total attenuation.

B. Application to Distributed Sensors

If longitudinal variations of Rayleigh scattering, fiber diameter, NA, or total loss can be induced in a fiber controllably by external effects, then it is clear that OTDR can be used to provide spatially resolved sensing. The fibers used should be designed deliberately to enhance their sensitivity to the quantity of interest. Each fiber may be seen as a continuous set of sensors, receiving the light in turn.

The remainder of this paper deals specifically with a distributed sensor which uses liquid-core fibers to provide a high sensitivity to temperature and a good immunity to other external factors such as mechanical perturbations. Preliminary results have recently been presented [17].

Of the fiber parameters which affect the backscatter signature, total loss is probably the easiest to make sensitive to temperature using, for example, changes in the strength, width, and position of absorption bands. A bulk device along these lines has been demonstrated recently [18] and, with suitable doping, fibers with similar properties could probably be developed. However, in a distributed sensor, modulation of the total loss

is undesirable since it imposes an unwelcome tradeoff between sensitivity and the amount of forward pulse energy available to probe the following sensing points. In addition, it is necessary then to differentiate the backscatter waveform to retrieve the temperature distribution and it follows that the requirements on the signal-to-noise ratio are very stringent if a reasonable resolution (e.g., a few meters) is to be achieved.

Variations of NA result from the difference between the thermooptic coefficients of the core and cladding materials. In glasses, these effects are normally so small as to be of no value; compositions specifically designed to enhance the sensitivity of the NA to temperature may become available in the future. In step-index multimode fibers a further, more fundamental, drawback exists namely that a reduction in NA between the source and the sensing point will act as a mode filter and can completely mask the local NA changes [16]. Thus sensing of the temperature at many positions in the fiber independently would be precluded. Note, however, that this is not the case in graded-index [10] or single-mode fibers [12] where NA variations may be detected all along the fiber using OTDR.

The remaining effect is that of changes in Rayleigh scattering. The latter shows some temperature sensitivity in glasses and is known to vary strongly in liquids [19]. Liquid-core fibers would thus appear to be an eminently suitable medium for a distributed temperature sensor. In addition, these fibers are likely to be largely immune to external influences other than temperature.

III. Temperature Sensing in Liquid-Core Fibers

A. Fabrication of Liquid-Core Fibers

Liquid-core fibers [20], [21] consist of a glass tube (the cladding) filled with an ultratransparent liquid of higher refractive index which forms the core. For the present work, silica capillary tubing was obtained by drawing silica tubes on a fiber-pulling machine to an outer diameter of 300 μm and to an inner diameter of 150 to 200 μm. Prior to the drawing, high-purity silica was deposited by the MCVD process on the inside of the tubes to reduce the loss of the cladding region. The capillary tubing was coated on-line with polyimide, a material which can be operated up to temperatures above 400°C. Polyimide has the further advantage that it is optically absorbing and hence acts as an effective continuous cladding-mode stripper. Cladding modes are known [22] to give rise to spurious effects in backscatter measurements and their total elimination is essential in this application.

The capillary tubing was filled with hexachlorobuta-1, 3-diene [20], [21] using a high-pressure syringe system. Typically, 150 m of 150-μm bore capillary can be filled in 30 min. It is important to prevent the incorporation of particulate matter in the core. Dirt particles form troublesome scatter centres which move as the temperature varies and as the liquid expands and contracts. A 0.2-μm pore filter in the syringe ensured that the fibers filled were free from scatter centres.

The fibers have an NA of 0.50 at $\lambda = 900$ nm ($\Delta = 5.5$ percent) and 0.54 at 589 nm. Their loss is typically 13 dB $\cdot$ km^{-1} at 900 nm as measured by the backscatter technique; lower losses have been reported with the same core liquid [21].

B. Operation

The configuration of the liquid-core temperature sensor is shown in Fig. 3. The source is typically a GaAs single-heterostructure laser emitting short (~10-ns) pulses of 1-2-W peak power at a wavelength of 900 nm. The laser output is focused through a beam splitter onto the end of a launch fiber which is held in an angled index-matching cell to eliminate the front-face reflection. The remote end of the launch fiber is inserted into the core of the sensing fiber and the joint thus formed is sealed. For the experiments to be described, the sensing fiber is arranged into three coils, two of which (A and C) are held at room temperature whereas the central fiber section (B) can be temperature-cycled.

The scattered light returning to the launching end is directed by the beam splitter via the collection optics to the Si avalanche photodiode detector. The photocurrent is fed to a 35-MHz bandwidth transimpedance preamplifier. The amplified signal is sent to a high-speed transient recorder where the data are stored and averaged before being transmitted to the computer for further processing.

Two major effects occur in a liquid-core fiber as its temperature is increased. First, the core refractive index is found to decrease. The temperature dependence of the refractive index of hexachlorobutadiene at $\lambda = 589$ nm is given by [24]

$$n(\Theta) = 1.5660 - 5.23 \times 10^{-4} \times \Theta \tag{3}$$

over the range $\Theta = 10$–75°C, where Θ is the temperature in Celsius. The fiber numerical aperture thus decreases strongly as the temperature is increased, which leads to a reduction of the backscatter signal.

The second effect is the increasing scattering loss, resulting from the increasing thermal agitation, and given by [19], [23]

$$\alpha_s(T) = \frac{8\pi^3}{3\lambda^4}\,(n_1^8\,p^2)\,kT\beta_T \tag{4}$$

where p is the photoelastic coefficient, k is Boltzmann's constant, T the absolute temperature, and β_T the isothermal compressibility. Since n_1, p, β_T all vary with temperature, α_s can have a large temperature sensitivity. In benzene, for example [19], the temperature sensitivity $d\alpha_s/dT$ is 0.033 dB $\cdot$ K^{-1}. The measurements on hexachlorobuta-1, 3-diene described in Section IV-B indicate a somewhat lower sensitivity of 0.022 dB $\cdot$ K^{-1} (to the author's knowledge, the temperature dependence of p and β_T for this compound have not been published).

Since the temperature sensitivity of the NA and of the scattering loss have opposing effects on the backscatter signal, one of these must be eliminated if the sensor is to be practicable. In the present work, the influence of NA variations is eliminated from the backscatter signal with the aid of a mode filter. These variations could not in any case be traced reliably along a step-index multimode fiber. The mode filter consists of a section of step-index multimode fiber, the NA of which is substantially lower than that of the liquid-core fiber. The filter, therefore, has the function of an angular stop and it transmits to the receiver backscatter power carried only in the low-order modes of the sensing fiber. NA variations affect the power content in the high-order modes only and these modes are lost at the mode filter. The mode filter thus elimi-

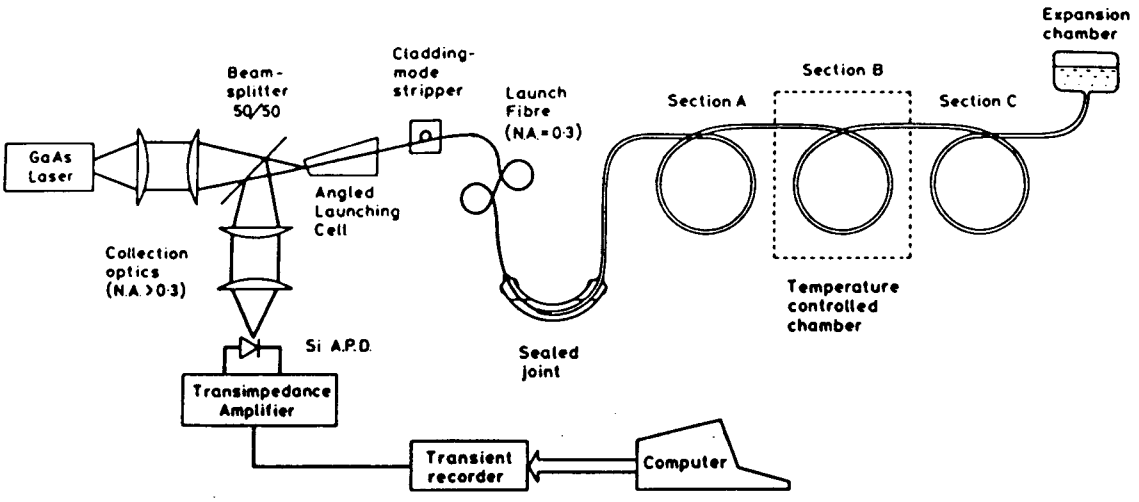

Fig. 3. Experimental arrangement for the distributed temperature sensor.

nates the sensitivity of the backscatter signal to changes in NA.

A small residual sensitivity to temperature-induced longitudinal index changes exists, however, since ray bending will occur at the interface between fiber sections at different temperatures, as illustrated in Fig. 4. This ray bending causes light scattered, say, in a relatively hot section (Fig. 4) to be converted from high-order to low-order modes and hence allows a larger proportion of the backscatter power to pass through the mode filter to the receiver. This residual effect fortunately has the same sense as the temperature dependence of scattering loss. It modifies the received backscatter signal by a factor of $(n_1(0)/n_1(z))^2$ and adds typically 1.5×10^{-3} dB · K^{-1} to the sensitivity of the sensor.

C. Design Study: Measurement Accuracy, Spatial Resolution, and Range

In this section, the potential performance of a liquid-core fiber sensor driven by a semiconductor laser is calculated. The numerical values of the important parameters are largely the same as those found in the experimental work (Section IV-A-D). The main difference is that it is assumed that an A/D converter is available to acquire and average the entire backscatter waveform at each laser pulse [25], [14], at a repetition rate of ~1 kHz. Although flash converters operating at 75 Megasample/s with 8-bit resolution are available commercially, a transient recorder with a maximum averaging rate of 20 waveforms/s was used in the present work. In addition, the laser pulse power was somewhat lower than has been assumed in the calculations.

1) Signal-to-Noise Ratio: Table I summarizes the properties of the components of the sensor system. The backscatter factor η can be evaluated from the properties of the fibers, with the aid of (2). The numerical aperture NA_R of the launch fiber, rather than that of the sensing fiber must be inserted in (2) since the former is the limiting NA in the receiving optics. The result is $\eta = 2.6 \times 10^3$ W/J at $\lambda = 904$ nm. The laser output pulse energy is 20 nJ.

Estimated losses L_T in the backscatter system are given in Table II for the complete path from the laser to the start of the sensing fiber and back to the receiver. These amount to 19 dB. The backscatter signal $P_r(x)$ from a point at distance x along the sensing fiber is, therefore,

$$P_r(x) = P_0 \, W \eta \, 10^{-(L_T + 2\alpha x)/10}. \tag{5}$$

Hence, for $x = 100$ m, $P_r(x) = 0.36$ μW. This optical signal is detected using an avalanche photodiode and a transimpedance amplifier. At the preamplifier output, the signal-to-noise ratio is approximated by [26]

$$S/N = \frac{(R P_r M)^2}{(2e(I_d + R P_r) M^2 + x_m + i_n^2) B} \tag{6}$$

where R, M, I_d, and x_m represent the responsitivity, avalanche gain, primary dark current, and excess noise factor of the photodiode, respectively. i_n is the equivalent input noise current of the preamplifier and B, its bandwidth; e is the electronic charge. Values for these parameters are given in Table I for the devices used in Part IV.

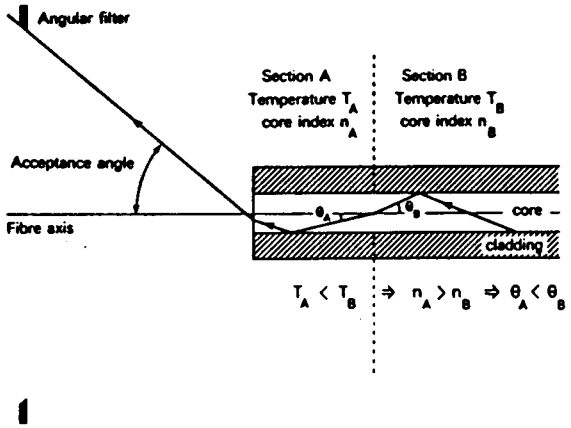

Fig. 4. Sensitivity of the mode-filter transmission to longitudinal variations of core index.

TABLE I
TYPICAL PROPERTIES OF THE COMPONENTS USED IN DISTRIBUTED TEMPERATURE SENSOR OPERATING AT A WAVELENGTH OF 0.9 μm

Component	Parameter	Symbol	Value
Laser	Peak Power	P_o	2W
	Pulse width	W	10^{-8}s
	Wavelength	λ_o	904nm
	Pulse repetition rate		1kHz
Sensing fibre	Total attenuation	α	13 dB/km
	Scattering loss	α_s	8.7 dB/km @ 20°C (2.0×10^{-3} np/m)
	(temp. coeff.)	$\frac{1}{\alpha_s}\frac{d\alpha_s}{dT}$	21.8 mdB/deg C
	Core diameter		150μm
	Outer diameter		300μm
	Core index	n_1	1.55 @ 20°C
	Group velocity	v_g	1.875×10^8 m/s @20°C
	Temperature sensitivity		23.3 mdB/deg C
Launch fibre	Length		10-50m
	Loss		<1dB
	Numerical Aperture	NA_R	.3
	Core diameter		100μm
	Outer diameter		140μm
Receiver	Detector responsivity	R	0.7 A/W
	Unmultiplied dark current	I_d	~0.2 nA
	Excess noise factor	x_m	0.35
	Input equivalent noise current	i_n	1.1 pA/Hz$^{\frac{1}{2}}$
	Bandwidth	B	35 MHz
	Transimpedance		10^5 Ω

TABLE II
LOSS BUDGET FOR THE OPTICAL PATH IN THE TERMINAL EQUIPMENT

Forward Path	
Beamsplitter	3dB
Reflections and aberrations	2dB
Launching efficiency	3dB
Loss of launch fibre	1dB
	9dB

Return Path	
Coupling loss	4dB
Launch fibre	1dB
Reflections and aberrations	2dB
Beamsplitter	3dB
	10dB

Total loss: 19dB

The optimum avalanche gain is obtained by differentiation of (6)

$$M_{\text{opt}} = \left[\frac{i_n^2}{x_m e(I_d + R P_r)}\right]^{1/(2+x_m)} \tag{7}$$

Substitution of M_{opt} into (6) gives the signal-to-noise ratio at optimum gain which, expressed as a voltage ratio, takes the value of 100 for the parameters given above. Assuming that the signal is averaged for 1 s (i.e., 1000 averages), the signal-to-noise ratio improves to $\sim 3 \times 10^3$. For a temperature sensitivity of 23×10^{-2} dB · K^{-1}, this signal-to-noise ratio leads to an uncertainty in the temperature of less than 0.1 °C (at 100 m).

If the temperature measurement is to be achieved to this degree of precision, attention must be given to the linearity of the receiver and data-acquisition system, and to the processing of the backscatter waveforms to extract the temperature information. The first point has been discussed in the literature [27], [28] and the second will be discussed in Section III-D.

2) Spatial Resolution: The spatial resolution of the sensor is directly related to the system impulse response, i.e., to the convolution of the pulse broadening in the fiber and the impulse response of the terminal equipment. Pulse propagation along a step-index fiber of length $2x$, results in a pulse broadening of [29]

$$\Delta\tau = \frac{x}{c}\frac{NA_R^2}{n_1} \tag{8}$$

provided that mode coupling can be neglected (c is the speed of light in free space). Pulse broadening places a fundamental limit to the sensor resolution which degrades linearly with distance, but can be controlled by restricting the receiving NA. At a distance of $x = 100$ m, receiving NA's of 0.1, 0.2, and 0.3 permit spatial resolutions of 0.2, 0.8, and 1.8 m, respectively. Although liquid-core fibers generally have very low mode conversion [30], the backscattering process itself will result in an almost complete redistribution of power amongst the mode groups. The figures given above are thus pessimistic, probably by as much as a factor of $\sqrt{2}$. The improvement in resolution achieved by restricting the receiving NA results in the signal-to-noise ratio being degraded in proportion to NA_R^4 since the launching efficiency into the launch fiber as well as the return coupling efficiency are reduced (owing to the mode conversion in the backscattering process it is necessary to restrict both the launching and receiving NA).

A similar compromise between spatial resolution and measurement accuracy exists in the measurement system, since any reduction in the laser pulsewidth decreases the backscatter signal, while increasing the bandwidth of the receiver will degrade its noise performance. Ideally, the impulse response of the fiber and of the receiver and the probe pulsewidth should all be of similar magnitude.

For the values given in Table I, the spatial resolution at a distance of 100 m is approximately 2.5 m. Suppose, however, that (at the same distance) a spatial resolution commensurate with the performance of a 75 Megasamples/s A/D converter, namely 1.25 m, is required. A probe pulsewidth and a fiber

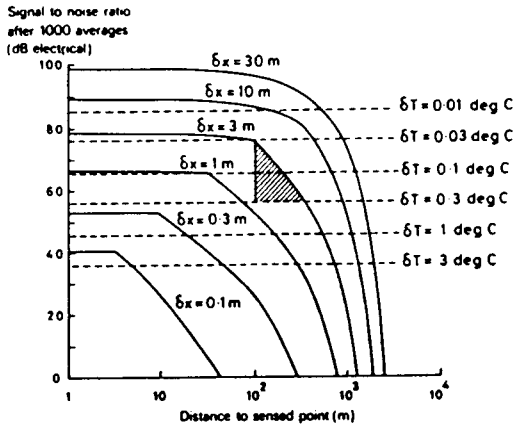

Fig. 5. Signal-to-noise ratio of the amplified backscatter signal as a function of position. Solid lines are calculated for various values of the spatial resolution δx. Broken lines show the signal-to-noise ratio required in order to obtain the temperature accuracy δT indicated.

impulse response of 7.7 ns or less and a receiver bandwidth of 60 MHz or more are needed to achieve it. It follows that, in each part of the system, parameter changes must be made, each of which results in a reduction to the signal-to-noise ratio. Thus it is estimated that the averaging time must be increased from 1 to ~16 s to preserve the signal-to-noise ratio after averaging.

Dispersion in the launch fiber can be reduced to negligible proportions by use of a graded-index fiber, at the expense of additional launching and coupling losses.

4) Range: It is clear from the foregoing that the performance of the sensor is a complicated function of the spatial resolution, the temperature measurement accuracy, and the maximum sensing distance which are required. In Fig. 5, the signal-to-noise ratio expected after averaging 1000 waveforms has been plotted as a function of the maximum sensing distance (solid lines). Each line is calculated for a different value of the spatial resolution δx required at the most remote sensing point. In each case, it is assumed that the sensor system is fully optimized for the desired operating condition and the consequences for the performance of the various components (e.g., coupling losses or amplifier equivalent input noise) have been included in the calculation.

For comparison, the broken lines indicate the signal-to-noise ratio needed to achieve given levels of accuracy in the temperature determination. For example, if a spatial resolution of <3 m at a distance of >100 m is needed, together with a temperature measurement accuracy of $<0.3°C$, then the sensor can be designed to operate anywhere within the shaded area on the figure. Similarly, it is possible to sense temperature to within 1°C at 100 m with a spatial resolution of 1 m. However, should a precision of 0.1°C be required at the same distance and for the same spatial resolution, then it would be necessary to perform more averaging, to use a higher power laser, or to improve the noise performance of the receiver.

D. Processing the Backscatter Waveform

The temperature sensitivity of the backscatter signal is, to first order, that of the scattering loss. In order to extract a valid temperature distribution from the measured backscatter waveform, corrections must be made for several other effects which also have a bearing on the shape of the signal. First, the temperature is determined from a power ratio and it is, therefore, important to acquire the baseline accurately. This may be achieved by measuring the signal after the backscatter has ceased. Similarly, in order to compensate for long-term drifts (e.g., of laser power) the entire waveform must be scaled to a power level external to the sensing fiber, for example, to the backscatter level in the solid-core fiber.

Core diameter variations produce fluctuations in η in proportion, for step-index fibers, to the change in core area [9], [16], [22]. In a fiber sensor such diameter variations will appear as spurious temperature nonuniformities. They can be corrected for, however, if the fiber is calibrated at a uniform temperature. Although fiber diameter control is now well understood [31], the drawing of hollow tubes to a constant diameter is much more difficult and it may be that this calibration step cannot be avoided. Fortunately, the tubes used in the present study appeared (from their backscatter traces) to have reasonably uniform bores.

Although temperature variations affect the received power $p(t)$ mainly via the coefficient α_s, the change in temperature also affects the overall loss of the fiber, which appears in the integrand in (1). Variations in the temperature distribution, integrated along the fiber, will result in a change in the loss to the sensing point. An error in the temperature reading is therefore produced for distant points. If the variation in fiber attenuation is due solely to a change in Rayleigh scattering, then a numerical integration of the temperature distribution up to the point of interest can be used to derive a correction factor. However, other contributions to loss, such as absorption are also likely to vary (perhaps unpredictably) with temperature, which would render the correction procedure inadequate. If backscatter waveforms measured from each end of the fiber are available, then longitudinal variations of η and α can be separated unambiguously using a technique first proposed by Di Vita and Rossi [8].

Finally, the group velocity in the sensing fiber is affected to a small extent by temperature changes and the locations corresponding to the time-samples will shift. This effect can be corrected completely adequately by computing the line integral of the temperature distribution between the launching end and the point of interest.

E. Networking of Distributed Sensors

The proposed sensors are intrinsically time-division multiplexed. In addition, the terminal equipment can be time-shared between a large number of fiber sensors using readily available coupling components. Several different configurations may be envisaged in which only one receiver is used. Multiple sources, independently triggered from the computer, are most appropriate since they ensure that no overlap between the various signals occurs. Alternatively, a single source could be used, in combination with power dividers and delay lines, at the expense of increased complexity and reduced signal-to-noise ratio.

The advantage of these multiplexing schemes is that the most expensive parts of the sensor system; namely, the data-

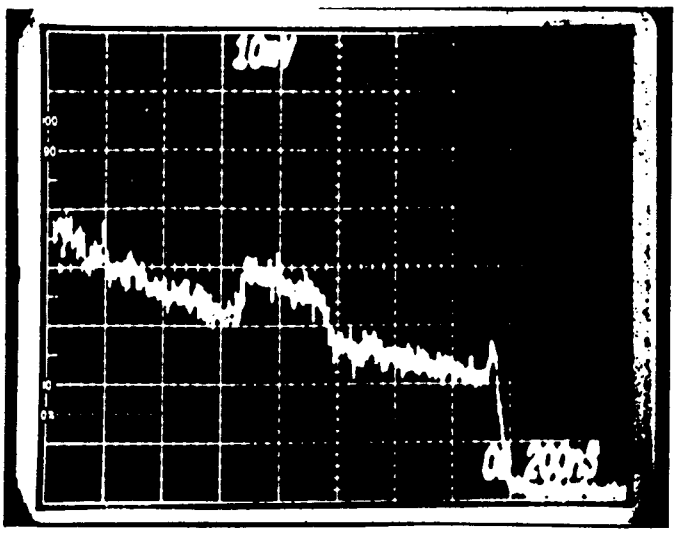

Fig. 6. Real-time backscatter waveform measured in the distributed temperature sensor. Time scale is 200 ns/div. The central section of the fiber is warmer by 33°C than the adjacent sections.

acquisition and processing equipment, is shared between sensors and this reduces the cost per sensing point of the system.

IV. Results and Discussion

A. Backscatter Waveforms in Liquid-Core Fibers

Backscatter measurements were made on liquid-core fibers fabricated as described in Section III-A using the experimental arrangement of Fig. 3.

Fig. 6 shows an oscilloscope trace of the backscatter signal returning from the remote end of a 170-m length of liquid-core fiber. The increase in signal which is clearly apparent between 600 and 1000 ns from the left-hand side is due to the corresponding fiber section being heated by ~33°C above that of the remaining fiber portions. The waveform shown was recorded without any signal averaging. Nevertheless, and in spite of the unusually high spatial resolution for OTDR, the signal-to-noise ratio is more than adequate to reveal the localized temperature increase, owing to the large backscatter factor of liquid-core fibers. Clearly, with only a moderate amount of signal averaging very small departures from temperature uniformity can be detected.

A range of similar waveforms are shown in Fig. 7. In each case, the central fiber section, section B, was at the temperature indicated, whereas the remaining sections, A and C, were held at room temperature (20°C). It is clear from the figure that the backscatter signal follows the local temperature variation, including when the temperature of section B falls below that of sections A and C.

In Fig. 8, the effect of a localized temperature increase on the backscatter signal has been emphasised by dividing the waveform by one measured while the fiber had a uniform temperature of 20°C. This is a simple means of correcting the waveform for the exponential decay associated with fiber loss and for the effect of diameter changes. It also gives an indication of the magnitude of the noise remaining after averaging and of any long-term drift. The waveform of Fig. 8 is the result of averaging 2500 measurements; it may be seen that the rms noise is less than 0.1 percent and that the normal-

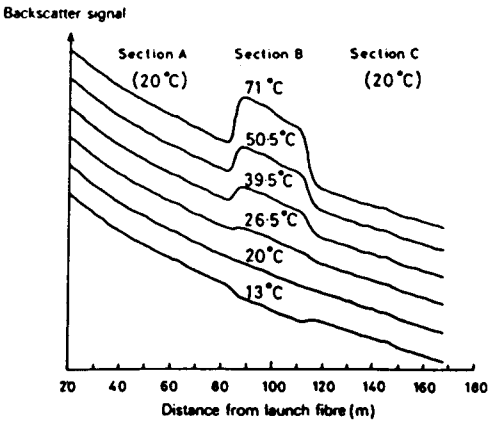

Fig. 7. Averaged backscatter waveforms measured in the liquid-core fiber with the temperature distributions indicated.

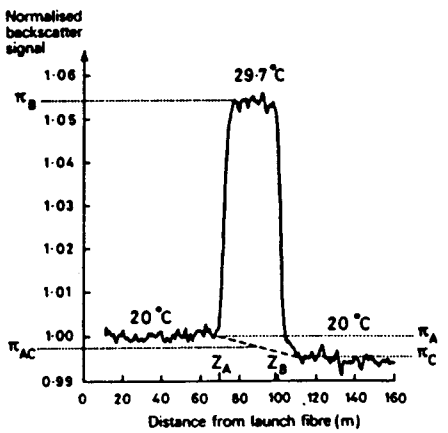

Fig. 8. Backscatter signal measured in the liquid-core fiber whose three zones were held at the temperatures indicated. The waveform has been normalized to a backscatter signal measured on the same fiber at a uniform temperature of 20°C.

ized signal in section A is very close to 1, which indicates that the long-term drift is small.

Two effects are now apparent, namely, the increase in backscatter from section B (which in this case is at a higher temperature than the rest of the fiber) and secondly the accompanying increase in scattering loss which results in a reduced signal level in section C. The latter is one of the effects which would normally be corrected in a fully engineered system by the separation of the true local attenuation and the backscatter factor.

π_A, π_B, and π_C are defined as the mean backscatter powers in regions A, B, and C, respectively, measured (as in Fig. 8) relative to the signal level found at the same point in the fiber at a uniform temperature of 20°C. These quantities have been indicated in the figure, as has the geometric mean π_{AC} of π_A and π_C.

For the simplified temperature distribution used in these experiments, the sensitivity of the device may be deduced from measurements of π_B/π_{AC} and the change in loss as a function of temperature is obtained from π_C/π_A.

B. Sensitivity Measurements in Fibers Having Low-Loss Claddings

The temperature sensitivity of a liquid-core fiber produced from a low-loss silica capillary tubing and filled with hexa-

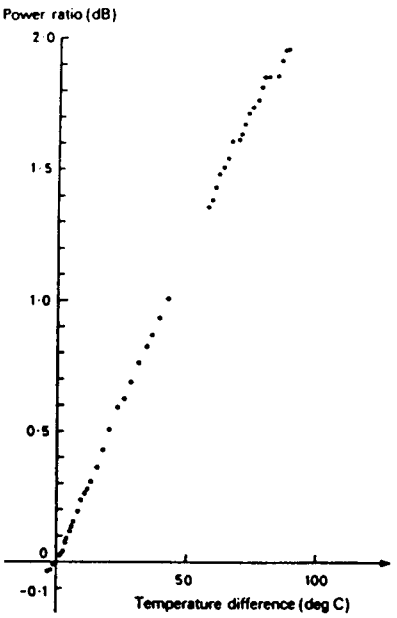

Fig. 9. Response of the sensor as a function of the departure of the temperature from 20°C.

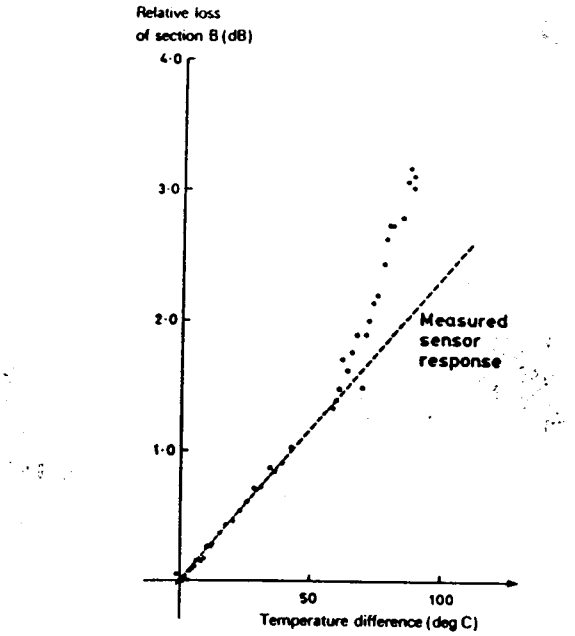

Fig. 10. Increase in loss of heated secion, relative to its loss at 20°C, as a function of the imposed temperature change (dots). The broken line is a least squares fit to the data of Fig. 9.

chlorobuta-1,3-diene is shown in Fig. 9. The results are given in the form of the power ratio π_B/π_{AC} as a function of the temperature difference ΔT. The relationship is linear and has a slope of 23.3×10^{-3} dB/°C over the range $\Delta T = -4$ to 88°C. The device is not restricted, in theory, to this range and the limits to the operating temperature are discussed in Section IV-E.

The temperature sensitivity of Rayleigh scattering in hexachlorobuta-1,3-diene may be estimated by subtracting the (calculated) contribution of the longitudinal index changes from the measured sensitivity of the backscatter signal. The result is 21.8×10^{-3} dB/°C. An independent estimate of the temperature coefficient of Rayleigh scattering is obtained from the change in loss of section B, π_C/π_A. For a direct comparison with the previously obtained temperature coefficient of α_s, π_C/π_A must be scaled to the room-temperature value of α_s and to the length of section B to give a relative temperature-dependent loss $\Lambda(T_B - T_0)$ defined by

$$\Lambda(T_B - T_0) = 10 \log_{10} \left[1 + \frac{\pi_C (T_B - T_0)}{2\pi_A (T_B - T_0)\alpha_s(T_0)(Z_B - Z_A)}\right] \quad (8)$$

where T_B is the temperature of interest, T_0 is room temperature, and $Z_B - Z_A$ is the length of section B. In Fig. 10, the quantity Λ is plotted (dots) as a function of the temperature difference $\Delta T = T_B - T_0$ (the ratio π_C/π_A is expressed in decibels). For comparison, the solid line is a least square fit to the sensitivity data of Fig. 9. In the region $\Delta T = 0$–60°C, the excess loss closely resembles the temperature sensitivity curve. This demonstrates that, as predicted in Section III-B, the sensitivity of the device is largely due to the contribution of Rayleigh scattering. A straight-line fit to the data of Fig. 10 gives a slope of 24.2×10^{-3} dB/°C. This result is somewhat higher than that obtained for the Rayleigh scattering (21.8×10^{-3} dB/°C). The difference is possibly due to the temperature sensitivity of absorption loss in the core liquid. However, the scattering loss $\alpha_s(T_0)$ in hexachlorobuta-1,3-diene is not known to sufficient accuracy for the discrepancy to be considered definitely significant. In any case, comparison of the two curves shows that liquid-core temperature sensors can be built which operate very near to the theoretically predicted sensitivity. This ensures that the sensitivity is very reproducible from one sensor to the next since it is determined only by the basic physical properties of the materials used.

As the temperature difference between fiber sections increases, however, the backscatter return from the hot zone carries an increasing proportion of power in high-order modes, since the NA of the hot zone is decreasing. In addition, the longitudinal refractive-index gradient serves slightly to increase the receiving NA for the hot zone which results in a further increase in the proportion of power carried by high-order modes. The two effects combined lead to the much larger gradient of $\Lambda(T_B - T_0)$ at temperature differences above $\Delta T = 60$°C. The temperature sensitivity of the device does not, however, appear to be affected until ΔT reaches 94°C, at least.

C. Effect of Differential Mode Attenuation (DMA) on the Performance of the Sensor

Although the results presented so far indicate that the sensitivity of the sensor is not significantly affected by the attenuation of high-order modes, the loss of heated sections clearly is. Thus DMA could potentially become a source of error in the distributed temperature sensor and its effects deserve investigation.

The effect of DMA may be studied by enhancing the loss of high-order modes or by using the mode filter to select high-order modes in the backscattered power.

In the latter approach, our objective may be achieved by cutting the end of the launch fiber at an angle markedly different from perpendicular to the axis, which causes ray bending at the liquid-glass interface. In our experiments, the fiber end was cut at an angle of 35° from the normal. Hence the power

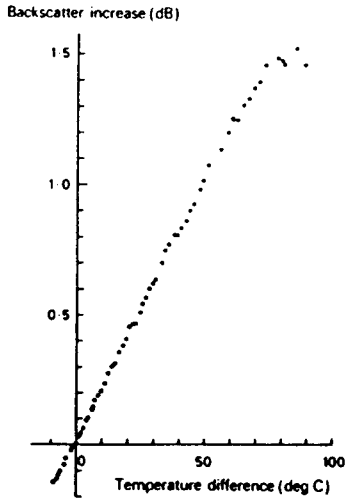

Fig. 11. Response of the temperature sensor when the launch fiber end is cut at an angle of 35° from normal to its axis.

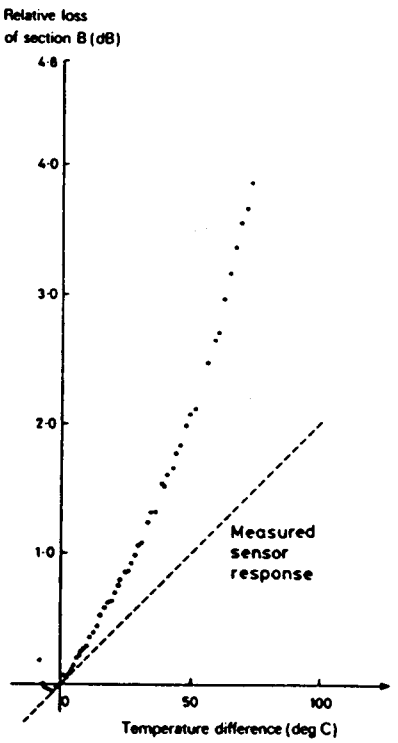

Fig. 12. Increase in loss of the heated section, relative to its loss at 20°C, as a function of the imposed increase in temperature (dots). The launch fiber is cut at an angle of 35° from normal to its axis. Broken line is fitted to the data of Fig. 11.

traveling at ~1.4° from the axis in the liquid-core fiber couples to the lowest order mode of the launch fiber. The receiver thus detects power which is still restricted to a maximum numerical aperture, but which is now biased towards a higher order mode content. Figs. 11 and 12 show, respectively, the sensitivity curve and A as functions of the temperature difference. In both cases, the effect of DMA on the sensor performance is obvious. Thus the sensitivity is now linear up to $\Delta T = 75°C$ only, since the NA of section B approaches that of the mode filter at lower temperatures than in the case of an end cut normal to the fiber axis. It is calculated that the NA of the liquid-core falls to the effective NA of the mode filter

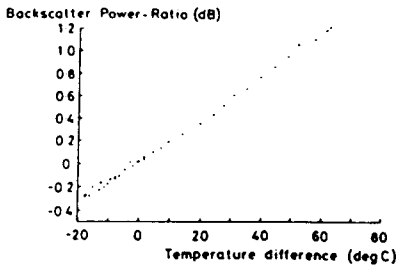

Fig. 13. Sensitivity curve of a liquid-core sensor having a lossy cladding.

at $\Delta T = 84°C$, allowing for the ray bending at the liquid-glass interface. The corresponding value is $\Delta T = 94°C$ for a launch fiber cut at right angles. This is confirmed experimentally, since, in Fig. 11, the power ratio ceases to increase for $\Delta T > \sim 80°C$. In addition, the sensitivity of the device has fallen by some 15 percent to 20.2×10^{-3} dB/°C. The reason for the lower sensitivity is clear from Fig. 12 which shows that the excess loss of section B is now much more sensitive to temperature for all values of the temperature difference.

The effect of the cladding loss and the associated DMA can be studied by using capillary tubes in which no low-loss cladding layers have been deposited. This type of fiber was used in the preliminary work [17]. The sensitivity curve for such a fiber is shown in Fig. 13. Again the curve is linear (in decibels) over the region -15 to +60°C. Its slope, however, is reduced to 18×10^{-3} dB/°C in contrast to the 23.3×10^{-3} dB/°C measured on fibers with low-loss claddings. In addition, it is found that the backscatter waveform is distorted by DMA at large temperature differences, as illustrated in Fig. 14. Trace (*a*) in the figure was obtained with $\Delta T = 27°C$. It is similar in appearance to waveforms obtained on fibers with low-loss claddings. For the second trace, trace (*b*), however, the temperature difference is 62°C and the backscatter waveform is clearly distorted. At the beginning of section B, a region of rapid decay now exists which corresponds to the rapid removal of the high-order mode contribution to the backscatter signal from this section. In addition, the apparent loss is reduced in the fiber section immediately following the heated part. DMA can, therefore, produce serious errors in the temperature reading.

In fibers with deposited low-loss claddings, errors resulting from DMA occur only within a few degrees of a "cutoff temperature" at which the NA of the hottest fiber section falls to that of the launch fiber. In this case, DMA results from the received signal containing modes almost at cutoff. For example, Fig. 15 shows a series of backscatter waveforms measured in a fiber with a low-loss cladding at various temperatures, all near the "cutoff temperature." In Fig. 15(a), the NA of the launch fiber is 0.3 and it may be seen that the shape of the waveforms become distorted for $\theta > 114°C$ and that the sensor loses all sensitivity when θ reaches 131°C. In Fig. 15(b), however, the waveforms were measured with a launch fiber of NA = 0.2 and it is found that the temperature at which distortion to the backscatter traces occurs is increased to ~140°C. The cutoff temperature may be calculated from the refractive index data for hexachlorobuta-1,3-diene and for fused silica, and the results are given in Table III for two values of an operating

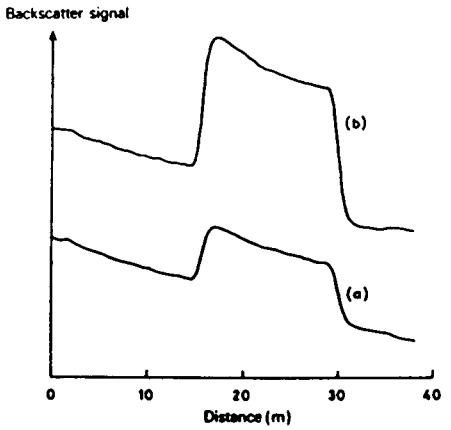

Fig. 14. Detail of backscatter waveforms measured in a liquid-core fiber having a lossy cladding. For trace (*a*), the temperature difference between the sections is 27°C and is 62°C for trace (*b*).

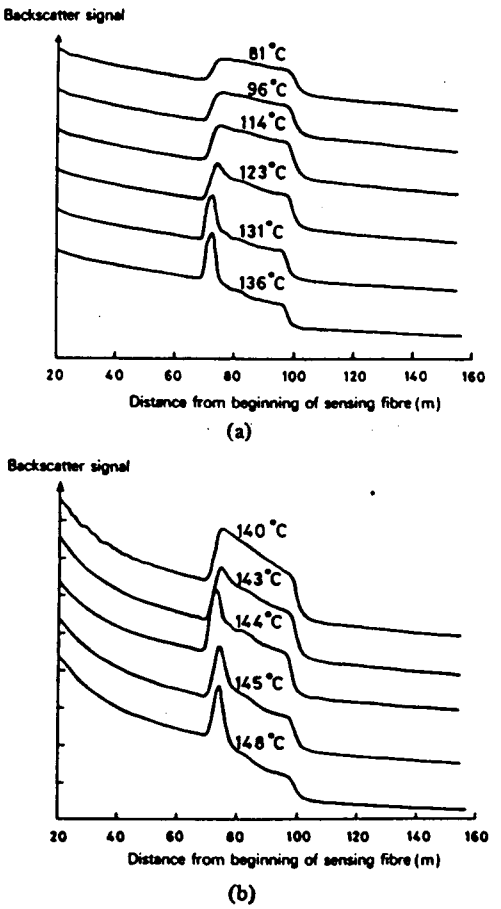

Fig. 15. Backscatter waveforms measured for large temperature differences on liquid-core fibers having low-loss claddings. (a) NA of launch fiber is 0.3. (b) NA of launch fiber is 0.2.

wavelength and of receiving numerical aperture. The values calculated for $\lambda = 900$ nm agree well with the observed behavior.

From the foregoing, DMA is clearly a potential source of inaccuracy in the temperature measurement. If, however, the CVD process is used to reduce the cladding loss, then the effect of DMA is largely eliminated over the entire operating range of the sensor. The measured sensitivity then correlates well with the change in loss in regions where the temperature is varied.

TABLE III
CUTOFF TEMPERATURES AT WHICH THE NUMERICAL APERTURE OF THE LIQUID-CORE FIBER FALLS TO THAT OF THE LAUNCH FIBER

Receiving NA \ Operating Wavelength	589nm	900nm
0.2	176 °C	144 °C
0.3	144 °C	112 °C

Similarly, for the angles at which the launch fiber end is expected to be broken, no significant DMA is likely to exist. Thus if the waveguide is prepared with care DMA has no significant effect on the operation of the sensor over a wide temperature range.

D. Effect of Cladding Modes on the Backscatter Waveform

Initial measurements in this study were made on fibers having a silicone primary coating. This type of structure naturally guides a large number of cladding modes which are able to reach the receiver and produce a spurious contribution to the backscatter via a variety of mechanisms such as imperfect mode filtering, scattering in the core, or mode conversion at diameter changes or bends. As a result, anomalous effects were observed, such as an increase in the backscatter signal at a variable-temperature section, regardless of whether the latter was heated or cooled. The experimental arrangement of Fig. 3 in which the launch fiber is inserted inside the core of the sensing fiber to form a joint automatically selects modes bound to the core since power in cladding modes traveling through the core always fall outside the NA of the launch fiber. This mode-filtering arrangement, in combination with an absorbing primary coating (such as polyimide) completely eliminates the problem of cladding modes which can otherwise severely affect the shape of the backscatter waveform [22]. Note that the scattering process itself sets a lower limit on the interchange of power between the modes of the core and the cladding. Fortunately, this presents no problem for the fiber lengths and scattering loss envisaged here.

E. Limits to the Temperature Range

The ultimate limitations to the temperature range are the freezing and boiling points of the core liquid. For hexachlorobuta-1,3-diene, the resulting temperature range would be -19 to 212°C, i.e., a substantially wider range than is available from other suitable low-loss liquids. In practice, however, the range is limited by other effects.

The maximum operating temperature is that at which the NA of the liquid-core fiber falls to that of the launch fiber. This effect is discussed in Section IV-C and Table III lists the maximum temperatures for different NA's and operating wavelengths. To some extent, the temperature range can be modified by a suitable choice of operating wavelength, receiving

NA, cladding index, and ultimately of core material. Note that, at the maximum temperature range, the local attenuation of the fiber increases abruptly with increasing temperature. This effect can be used as an "alarm" to indicate that, at a particular point along the fiber, the temperature has reached a dangerous level. The ability to vary the alarm temperature is thus of considerable advantage.

The operating temperature is further limited by damage, which occurs if the fiber is heated to about 160°C. The attenuation of the overheated section is found to suffer from an irreversible increase in absorption loss. Damage is also caused by exposure to ultraviolet light—an occurance which is fortunately relatively easily prevented.

At low temperatures, the range is, surprisingly, limited by the fiber loss increasing with decreasing temperature. Although this mechanism is not at present understood, it appears to be associated with the heating damage already mentioned, since the temperature at which the excess loss becomes noticeable is increased after the fiber has been exposed to high temperatures.

In the present study, the range 5 to 110°C was covered. With further attention to eliminating DMA and to damage, a significant improvement in range is anticipated. An attractive possibility is to use more robust a liquid such as C_2Cl_4 [32], which is liquid over the range - 22 to 121°C.

V. Conclusions

Optical fiber sensors of a new type have been proposed; they are able to monitor remotely the spatial distribution of the physical parameter of interest. The sensors use OTDR to detect externally induced changes in the backscatter signature of specially designed optical fibers.

A design study and performance calculations have been presented for a distributed temperature sensor which uses a liquid-core fiber as the sensitive medium. The analysis shows that, for presently available components, the sensor is capable of a resolution of 1 m over fiber lengths of more than 100 m, with a temperature accuracy of 1°C.

Experimentally, fibers consisting of hexachlorobuta-1,3-diene cores and silica cladding were found to have a sensitivity of 23.3×10^{-3} dB/°C (0.54 percent $°C^{-1}$) over the temperature range 5-110°C. The sensitivity measured results primarily from the increase in Rayleigh scattering coefficient with increasing temperature and this was confirmed by measurements of the temperature-induced excess loss.

The effect of DMA on sensor performance was investigated and it was found to be negligible provided that the fibers have low-loss claddings and that a suitable mode filter is placed in front of the receiver. Similarly, any detrimental effect of cladding modes can be eliminated very simply by use of a lossy primary coating and of a mode filter.

The device which has been described has a sufficient sensitivity and range to be useful in many situations in which the temperature must be monitored at many points simultaneously. Liquid-core fibers suffer from several drawbacks such as their susceptibility to damage and impurity ingression, which can be overcome by careful engineering. Owing to the simple construction of liquid-core fibers, the performance of the devices is expected to be extremely reproducible. Finally, it is hoped that in future solid core fibers with a usable sensitivity may become available.

Acknowledgment

The author is indebted to R. J. Mansfield for producing the capillary tubes used in this study, to E. J. Tarbox, S. R. Norman, and M. P. Gold for many useful discussions, to D. N. Payne for advice and encouragement during the work, and to W. A. Gambling for his guidance.

References

[1] T. G. Giallorenzi, J. A. Bucaro, A. Dandridge, G. H. Sigel, J. H. Cole, S. C. Rashleigh and R. G. Priest, "Optical fiber sensor technology," *IEEE J. Quantum Electron.*, vol. QE-18, pp. 626-665, 1982.

[2] A. L. Harmer, "Principles of optical fiber sensors and instrumentation," *Meas. Contr.*, vol. 15, pp. 143-151, 1982.

[3] M. Gottlieb and G. B. Brandt, "Fiber-optic temperature sensor based on internally-generated thermal radiation," *Appl. Opt.*, vol. 20, pp. 3408-3417, 1981.

[4] —, "Temperature sensing in optical fibers using cladding and jacket loss effects," *Appl. Opt.*, vol. 20, pp. 3867-3873, 1981.

[5] J. P. Dakin and D. A. Kahn, "A novel fiber-optic temperature probe," *Opt. Quant. Electron.*, vol. 9, pp. 540-544, 1977.

[6] M. K. Barnoski and S. M. Jensen, "Fiber-waveguides: A novel technique for investigating attenuation characteristics," *Appl. Opt.*, vol. 15, pp. 2112-2115, 1976.

[7] S. D. Personick, "Photon probe—An optical time-domain reflectometer," *Bell Syst. Tech. J.*, vol. 56, pp. 355-367, 1977.

[8] P. Di Vita and U. Rossi, "The backscattering technique: Its field of applicability in fiber diagnostics and attenuation measurements," *Opt. Quant. Electron.*, vol. 11, pp. 17-22, 1980.

[9] A. J. Conduit, D. N. Payne, and A. H. Hartog, "Optical-fiber backscatter-loss signature: Identification of features and correlation with known defects using the two-channel technique," in *Proc. 6th European Conf. on Optical Communication* (York, UK), 1980, pp. 152-155.

[10] M. Eriksrud and A. R. Mickelson, "Experimental investigation of variation of backscatter power with numerical aperture in multimode optical fibers," *Electron. Lett.*, vol. 18, pp. 130-132, 1982.

[11] N. Shibata, M. Tateda, S. Seikai, and N. Uchida, "Measurements of waveguide structure fluctuations in a multimode optical fiber by backscattering technique," *IEEE J. Quantum Electron.*, vol. QE-17, pp. 39-43, 1981.

[12] M. P. Gold and A. H. Hartog, "Determination of structural parameter variations in single-mode optical fibers by time-domain reflectometry," *Electron. Lett.*, vol. 18, pp. 489-490, 1982.

[13] A. J. Rogers, "Polarization optical time-domain reflectometry," *Electron. Lett.*, vol. 16, pp. 489-490, 1980.

[14] A. H. Hartog, D. N. Payne, and A. J. Conduit, "Polarization optical time-domain reflectometry: Experimental results and application to loss and birefringence measurements in single-mode optical fibers," in *Proc. 6th European Conf. on Optical Communication* (post-deadline paper, York, UK), 1980.

[15] E. G. Neumann, "Theory of the backscattering method for testing optical fiber cables," *Arch. Elek. Übertragung.*, vol. 34, pp. 157-160, 1980.

[16] A. R. Mickelson and M. Eriksrud, "Theory of the backscattering process in multimode optical fibers," *Appl. Opt.*, vol. 21, pp. 1898-1909, 1982.

[17] A. H. Hartog and D. N. Payne, "Remote measurement of temperature distribution using an optical fiber," in *Proc. 8th European Conf. on Optical Communication* (Cannes, France), 1982, pp. 215-220.

[18] K. Kyuma, S. Tai, T. Sawada, and M. Nunoshita, "Fiber-optic instrument for temperature measurement," *IEEE J. Quantum Electron.*, vol. QE-18, pp. 676-679, 1982.

[19] I. L. Fabelinskii, *Molecular Scattering of Light*. New York: Plenum, 1968.

[20] D. N. Payne and W. A. Gambling, "New low-loss liquid-core fiber waveguide," *Electron. Lett.*, vol. 8, pp. 374-376, 1972, see also U.S. Patent 3 894 788.

[21] —, "The preparation of multimode glass and liquid-core optical fibers," *Opto-Electron.*, vol. 5, pp. 297-307, 1973.
[22] A. J. Conduit, D. N. Payne, A. H. Hartog, and M. P. Gold, "Optical fiber diameter variations and their effect on backscatter loss measurements," *Electron. Lett.*, vol. 17, pp. 307-308, 1981.
[23] D. A. Pinnow, T. C. Rich, F. W. Ostermayer, and M. DiDomenico, "Fundamental optical attenuation limits in the liquid and glassy state with application to fiber optical waveguide materials," *Appl. Phys. Lett.*, vol. 22, pp. 527-529, 1973.
[24] S. R. Norman, private communication, 1974.
[25] R. D. Jeffery and J. L. Hullett, "N-point processing of optical fiber backscatter signals," *Electron. Lett.*, vol. 16, pp. 822-823, 1980.
[26] H. Melchior, M. B. Fisher, and F. R. Arams, "Photodetectors for optical communications systems," *Proc. IEEE*, vol. 58, pp. 1466-1486, 1970.
[27] A. J. Conduit, J. L. Hullett, A. H. Hartog, and D. N. Payne, "An optimised technique for backscatter attenuation measurements in optical fibers," *Opt. Quant. Electron.*, vol. 12, pp. 169-178, 1980.
[28] J. L. Hullett and R. D. Jeffery, "Long-range optical fiber backscatter loss signatures using two-point processing," *Opt. Quant. Electron.*, vol. 14, pp. 41-49, 1982.
[29] D. Gloge, "Weakly-guiding waveguides," *Appl. Opt.*, vol. 10, pp. 2251-2258, 1971.
[30] W. A. Gambling, D. N. Payne, and H. Matsumura, "Pulse dispersion for single-mode operation of multimode cladded optical fibers," *Electron. Lett.*, vol. 10, pp. 148-149, 1974.
[31] M. R. Hadley, D. N. Payne, and R. J. Mansfield, "Identification of sources of diameter fluctuations in smooth optical fibers by analysis of their spatial power spectrum," in *Proc. 6th European Conference on Optical Communication* (York, UK), 1980, pp. 53-56.
[32] J. Stone, "Optical transmission in liquid-core quartz fibers," *Appl. Phys. Lett.*, vol. 20, pp. 239-240, 1972.
[33] G. J. Ogilvie, R. J. Esdaile, and G. P. Kidd, "Transmission loss of tetrachloroethylene-filled liquid-core-fiber light guide," *Electron. Lett.*, vol. 8, pp. 533-534, 1972.

*

Arthur H. Hartog received the B.S. degree in electronics and the Ph.D. degree from the University of Southampton, Southampton, England, in 1976 and 1981, respectively.

He was a Research Student with the Optical Fiber Group at Southampton University, and later became a Research Fellow. He has studied propagation in optical fibers, including material and intermodal dispersion, and the OTDR and POTDR techniques for fiber evaluation.

Dr. Hartog was awarded the 1979 John Logie Baird Traveling Scholarship by the Royal Television Society.

0733-8724/83/0900-0509$01.00 © 1983 IEEE